

A LOW-TEMPERATURE X-RAY DIFFRACTION STUDY OF THE $\text{Cu}_2\text{ZnSnSe}_4$ THIN FILMS ON A MO FOIL SUBSTRATE

A.V. Stanchik¹, V.A. Chumak¹, V.F. Gremenok¹, S.M. Baraishuk², T.V. Shoukavaya¹

¹State Scientific and Production Association

«Scientific-Practical Materials Research Centre of the National Academy of Sciences of Belarus»

220072, Minsk, 19, P. Brovka str., Belarus, e-mail: alena.stanchik@bk.ru

²Belorussian State Technical Agrarian University,

220023, Minsk, 99, Nezavisimosti Av., Belarus, e-mail: baraishuksm@gmail.com

ABSTRACT: The Zn-rich and Cu-poor $\text{Cu}_2\text{ZnSnSe}_4$ (CZTSe) thin films were produced on flexible Mo foil by the three-step process. The XRD analysis demonstrates that the film mainly consists of CZTSe tetragonal phase and can contain ZnSe secondary phase. In addition, there are reflections of Mo and MoSe_2 . It was found that the crystal structure of the CZTSe films deposited on a Mo foil substrate was stable at low temperatures. The lattice parameters a and c are linearly decreasing in rang 5.707–5.637 and 11.394–11.298 Å, respectively, with a change in the temperature of the X-ray measurements from the 300 to 100 K. The thermal expansion coefficient is $9.87 \times 10^{-6} \text{ K}^{-1}$.

Keywords: CZTSe, Flexible Substrate, Stability, Thin Film

1 INTRODUCTION

Flexible solar cells are very attractive because of their low cost potential and many application possibilities. Today, the most efficient solar cells are based on $\text{Cu}(\text{In,Ga})\text{Se}_2$ (CIGS) thin films deposited on metal foils (17.9% [1]). However, the expensive rare and toxicity components in CIGS place a great limitation to their capacity to provide world's energy require. Lately, the $\text{Cu}_2\text{ZnSnSe}_4$ (CZTSe) thin films have attracted considerable interest for applications in flexible solar cells due to their appropriate direct band gap, abundant and low-toxicity components [2]. Flexible solar cells with efficiencies as high as 7% have already been achieved using the CZTSe thin films [3]. It is important for the CZTSe crystal structure to be stable at temperature changes for better cell efficiency. Since it was shown that the transition from the ordered to disordered kesterite structure of CZTSe occurs at a temperature of 200 °C [4]. According to Scragg et al. [5], the partial disordering of Cu and Zn atoms in the (disordered) kesterite structure is a critical contribution to the band gap fluctuations, which is the reason for the low value of the open-circuit voltage (Voc) and, consequently, the efficiency of solar cells. Therefore, it is important to study the CZTSe films under various temperature conditions. Today, the CZTSe thin films are relatively well studied by XRD and Raman spectroscopy at high temperatures compared to a low temperature. The purpose of this work is to study the behavior of the crystal structure of the CZTSe thin films deposited on a Mo foil in the temperature range from 100 to 250 K by XRD.

2 EXPERIMENTAL

2.1 Synthesis of the CZTSe thin films

The CZTSe thin films were produced by selenization of the deposited precursors Cu/Sn/Zn [6,7]. The Cu/Sn/Zn precursors were electrochemically deposited on a Mo foil substrate in galvanostatic mode with the sequence of Cu, Sn and Zn layers. Preliminary annealing of the electrodeposited Cu/Sn/Zn precursors in a tube furnace in an 95% Ar + 5% H_2 atmosphere at 350 °C for 30 min was carried out. Then the Cu/Sn/Zn precursors were selenized in a home-made quartz container (volume ~13 cm³) with

5 mg of powdery Se under 1 bar of Ar gas pressure. Selenization was performed at 580 °C for 30 min.

2.2 Characterization

The SEM and EDS of the CZTSe thin films were carried out in a dual beam system FE-SEM-FIB Helios Nanolab 650 (FEI Company) equipped with an X-ray spectrometer X-Max (Oxford Instruments). The topography of the CZTSe films was investigated using a Microtestmachines NT 206 atomic-force microscope operating in the contact mode.

The structural behavior of the CZTSe films was studied in an TUR-62M X-ray diffractometer fitted with Rigaku low-temperature camera. The diffraction patterns were recorded using a $\text{CuK}_{\alpha 1}$ radiation ($\lambda = 0.154178 \text{ nm}$) with a step of 0.03° and 3 s exposition. A copper-constants thermocouple was used for measuring the temperature of the sample. The XRD patterns were recorded in the temperature range 100–250 K at the interval of 50 K in vacuum. Analysis of the phase composition was performed with the Crystallography Open Database (COD) by «Match» software package. The Rietveld analysis implemented in the «Material Analysis Using Diffraction» («MAUD») software package was used for determination of lattice parameters of the CZTSe films.

3 RESULTS AND DISCUSSION

3.1 Composition and morphology

The elemental composition of the CZTSe thin films is represented in Table 1. The ratios of $\text{Cu}/(\text{Zn}+\text{Sn})$ and Zn/Sn indicates a deficiency of copper and an excess of zinc in the CZTSe thin films. It should be noted that the elemental composition of the obtained CZTSe films on Mo foil corresponds to the criterion of high-efficiency solar cells based on the CZTSe thin films [2].

The micrograph of the CZTSe thin film (Fig. 1) shows two types of crystals. The small crystals have the size of about 27 nm and the size of large crystals is more than one micron. The thickness of the CZTSe layer is about 2 μm. In addition, on the micrograph of the cross section of CZTSe film, we can see MoSe_2 layer at the interface between the Mo substrate and the CZTSe layer. The formation of MoSe_2 layer is a consequence of the high Se vapor pressure in the chamber during annealing of the

films and it is inevitable. The formation of a thin MoSe₂ layer is important consequences on device performance. It is suggested that a thin MoSe₂ layer facilitating a quasi-ohmic contact and good adhesion with the absorber film when its thickness is less than a few hundred nanometers [8]. For example, a thickness of the MoSe₂ layer is 0.9 μm in solar cells based on the CZTSe thin films with an efficiency of more than 11% [8].

Table I: The elemental composition and atomic ratio of the CZTSe thin films

Elemental composition, at %				Ratio	
Cu	Zn	Sn	Se	Cu/(Zn+Sn)	Zn/Sn
25.1	15.4	10.1	49.4	0.98	1.51

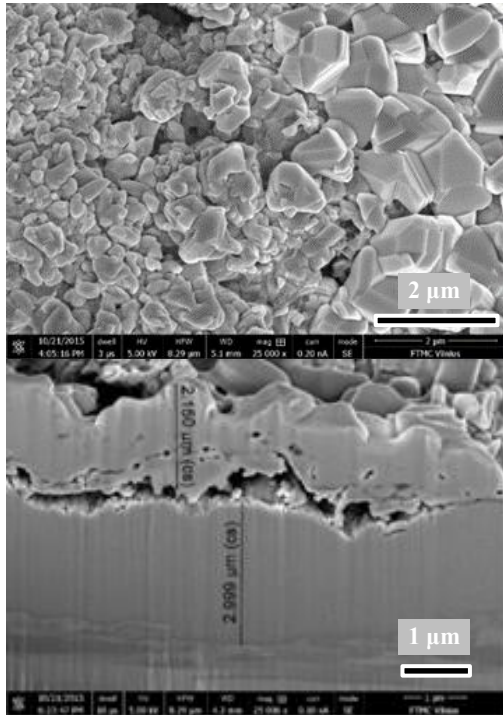


Figure 1: The micrograph of the CZTSe thin film on a Mo foil substrate

The AFM (2D and 3D) images of the CZTSe thin film deposited on a Mo foil are shown in Fig. 2. The surface of the films shows big and small grains of several 6×7.2 and 1×1.1 μm of 280 nm height, respectively, and with deep gaps between them. The root mean square and arithmetic roughness of surface the CZTSe film were determined to be 112 and 144 nm, respectively.

3.2 X-ray diffraction

The XRD patterns of the CZTSe thin films obtained in the temperature range 100–250 K were shown in Fig. 3. By comparing the XRD patterns it is seen that peaks have appeared at $2\theta = 27.1, 31.7, 36.2, 43.0, 45.3, 53.7, 56.2,$ and 65.9° belonging to the reflection of the planes (112), (020)/(004), (121), (123), (220)/(204), (312), (224), and (040)/(008), respectively, of the tetragonal structure of CZTSe (COD card No: 96-722-0527). In the XRD patterns, there are also reflections from Mo substrate (COD card No: 96-900-8544) and MoSe₂ layer (COD card No: 00-077-1715). These results agree well with the XRD analysis of the CZTSe thin films at room temperature (RT) [9]. However, the ZnSe as a secondary phase was probably existed in CZTSe films since the peaks of ZnSe (COD card

No:00-037-1463) are coincide with or very close to the peaks of CZTSe. The existence of ZnSe phase in films was confirmed by Raman spectroscopy in our earlier report [9].

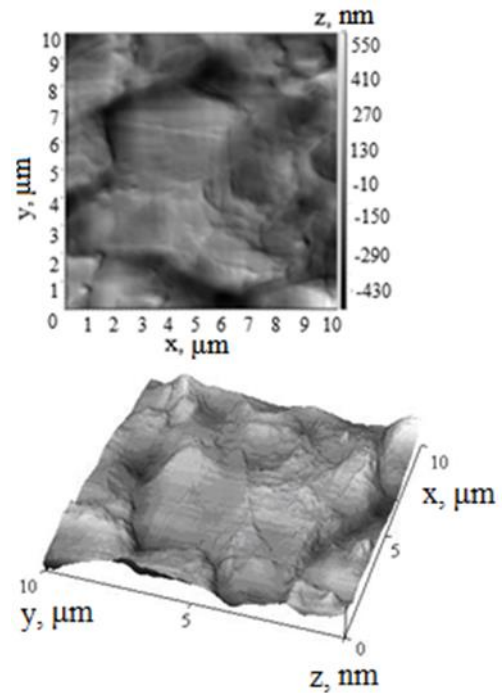


Figure 2: The AFM (2D and 3D) images of the CZTSe thin film on a Mo foil substrate

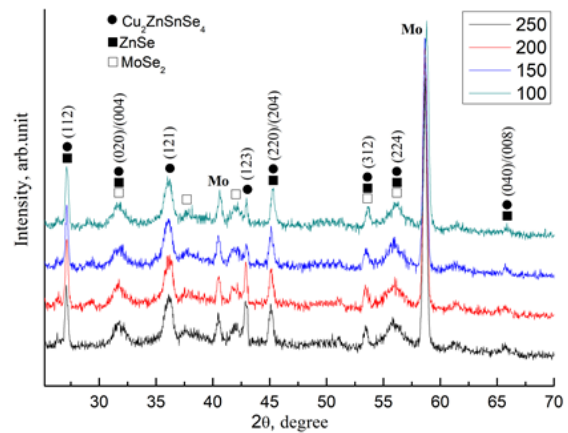


Figure 3: XRD patterns of the CZTSe thin film in the temperature range 100–250 K

From Fig. 3 it can be seen that all peaks are shifted towards lower angles with a change in the measurement temperature from 100 to 250 K. The lattice parameters are linearly decreasing with a change in the temperature of the X-ray measurements from the room temperature (RT) to 100 K (Fig. 4). The obtained data of the structural behavior of the CZTSe films deposited on a Mo foil substrate are in good agreement with the structural behavior of CZTSe single crystals at low-temperature [10].

The coefficients of linear thermal expansion of the CZTSe thin films were determined from the lattice parameters at five different temperatures ranging 100–300 K. The coefficients of linear thermal expansion were calculated using Eq. (1) and (2).

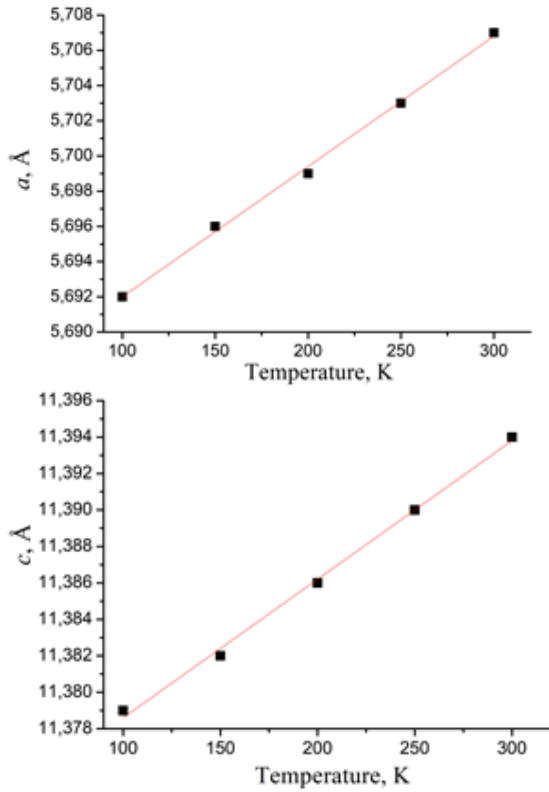


Figure 4: Temperature dependences of the lattice parameters a and c of the CZTSe thin film

$$\alpha_a = (a_T - a_{300})/a_{300}(T - 300) \quad (1)$$

$$\alpha_c = (c_T - c_{300})/c_{300}(T - 300) \quad (2)$$

where a_T and c_T are the lattice parameter at 100 K, a_{300} and c_{300} are the lattice parameter at 300 K.

The thermal expansion coefficients α_a and α_c are $13.2 \times 10^{-6} \text{ K}^{-1}$ and $6.59 \times 10^{-6} \text{ K}^{-1}$, respectively. The average coefficient of linear thermal expansion is therefore $9.87 \times 10^{-6} \text{ K}^{-1}$, which is almost the same as the linear thermal expansion calculated using the data without the room temperature ($9.64 \times 10^{-6} \text{ K}^{-1}$). The linear thermal expansion value was compared to the published value of $5.4 \times 10^{-6} \text{ K}^{-1}$ [10] and $8.4\text{--}8.6 \times 10^{-6} \text{ K}^{-1}$ [11]. The linear thermal expansion calculated using X-ray diffraction is found to be about twice as much as than the published value for the CZTSe single crystals [10] and almost closed to value for the CZTSe thin films grown on a Ti foil [11].

4 CONCLUSIONS

In this work, the CZTSe thin films were produced on a flexible Mo foil by the three-step process. The phase analysis of the CZTSe films at 100–300 K shows the presence of $\text{Cu}_2\text{ZnSnSe}_4$ basic phase and ZnSe secondary phase. It was found that the crystal structure of the CZTSe thin films deposited on a Mo foil substrate was stable at low temperatures. From the data of XRD analysis, the lattice parameters of CZTSe were determined. The lattice parameters a and c are linearly decreasing in rang 5.707–5.637 and 11.394–11.298 Å, respectively, with a change in the temperature of the X-ray measurements from the 300 to 100 K. The coefficient of linear thermal expansion of the CZTSe films calculated using X-ray diffraction is $9.87 \times 10^{-6} \text{ K}^{-1}$.

5 ACKNOWLEDGMENTS

This work was supported by Belarusian Republican Foundation for Fundamental Research (project T19M-022 and F20M-096).

6 REFERENCES

- [1] T. Yagioka, T. Nakada, Applied Physics Express Vol. 2 (2009) 072201.
- [2] M.P. Paranthaman, W. Wong-Ng, R.N. Bhattacharya, Semiconductor Materials for Solar Photovoltaic Cells (Springer International, Switzerland, 2016), Vol. 218, p. 25.
- [3] J.H. Sim, K.J. Yang, XXVI International Materials Research Congress (2017) P. SB.6-P031.
- [4] L.T. Schelhas, K.H. Stone, S.P. Harvey, D. Zakhidov, A. Salleo, G. Teeter, I.L. Repins, M.F. Toney, Phys. Status Solidi B, Vol. 254, 9 (2017) 1700156.
- [5] J.S. Scragg, J.K. Larsen, M. Kumar, C. Persson, J. Sandler, S. Siebentritt, C.P. Björkman, Physica status solidi. B, Vol. 253, 2 (2015) 247–254.
- [6] A.V. Stanchik, M.S. Tivanov, I.I. Tyukhov, R. Juskenas, O.V. Korolik, V.F. Gremenok, A.M. Saad, A. Naujokaitis, Solar Energy, Vol. 201 (2020) 480–488.
- [7] K. Urazov, M. Dergacheva, V. Gremenok, A. Stanchik, S. Bashkirov, Materials Today: Proceedings, Vol. 5 (2018) 22791–22797.
- [8] C. Platzer-Björkman, N. Barreau, M. Bär, L. Choubac, L. Grenet, J. Heo, T. Kubart, A. Mittiga, Y. Sanchez, J. Scragg, J. Phys Energy, Vol. 1 (2019) 044005.
- [9] A.V. Stanchik, V.F. Gremenok, S.A. Bashkirov, M.S. Tivanov, R.L. Juskenas, G.F. Novikov, R. Giraitis, A.M. Saad, Semiconductors, Vol. 52, 2 (2018) 215–220.
- [10] A.U. Sheleg, V.G. Hurtavy, V.A. Chumak, Crystallography reports, Vol. 60, 5 (2015) 758–762.
- [11] S. Yazici, M.A. Olgar, F.G. Akca, A. Cantas, M. Kurt, G. Aygun, E. Tarhan, E. Yanmaz, L. Ozyuzer, Thin Solid Films, Vol. 589 (2015) 563–573.